Journal of Photochemistry and Photobiology A: Chemistry 210 (2010) 209–214

Contents lists available at ScienceDirect

Journal of Photochemistry and Photobiology A: Chemistry

journal homepage: www.elsevier.com/locate/jphotochem

# Electron energy factors in photocatalytic methylviologen reduction in the presence of semiconductor nanocrystals

Olexandr L. Stroyuk*, Olexandra Ye. Rayevska, Andriy V. Kozytskiy, Stepan Ya. Kuchmiy

*L.V. Pysarzhevskiy Institute of Physical Chemistry of Ukr. Nat. Acad. Sci., 31 Nauky av., 03028 Kyiv-28, Ukraine*

ARTICLE INFO

*Article history:*
Received 24 September 2009
Received in revised form
23 November 2009
Accepted 26 November 2009
Available online 2 December 2009

*Keywords:*
Semiconductor nanocrystals
Photocatalysis
Methylviologen
Zinc oxide
Cadmium-zinc sulfide
Cadmium selenide
Photoluminescence
Charge traps

ABSTRACT

A linear relationship between the conduction band potential of a number of semiconductor nanocrystals ($Cd_xZn_{1-x}S$, CdSe, CdTe, ZnO) and the quantum efficiency of the photocatalytic methylviologen ($MV^{2+}$) reduction was found. It reflects dependence between the rate of photoinduced electron transfer from a semiconductor nanophotocatalyst to methylviologen and the overpotential of this process and is not affected by variations in chemical composition of the photocatalytic system.

Cadmium selenide nanocrystals were found to have photocatalytic properties in the $MV^{2+}$ reduction by sodium sulfite. Differences in the photoprocess kinetics observed for CdSe and $Cd_xZn_{1-x}S$ nanocrystals indicate that simultaneous photocatalytic reduction of $MV^{\bullet+}$ to $MV^0$ takes place in the case of cadmium selenide. Low efficiency of this process for $Cd_xZn_{1-x}S$ nanocrystals was interpreted as a result of lowering of the energy of photogenerated electrons due to the surface trapping. The results presented show that the availability, nature, and depth of surface charge traps of a nanophotocatalyst should be taken into consideration when interpreting the kinetics of photocatalytic processes with the participation of semiconductor nanocrystals.



## 1. Introduction

A special place among the photocatalytic reactions with the participation of organic substrates and semiconductor nanocrystals (NCs) belongs to the photocatalytic reduction of viologen-derivatives of 4,4′-dimethyldipyridyl. The most popular viologen-cationic methylviologen ($MV^{2+}$) can adsorb on the surface of semiconductor NCs and act as an acceptor of the conduction band electrons interfering with the electron–hole recombination in NCs. The product of the one-electron reduction of $MV^{2+}$ (the cation-radical $MV^{\bullet+}$) can further transfer electron to other components of the photo-catalytic system. In this way, $MV^{2+}$ functions as an electron mediator accelerating the interfacial charge transfer and the photocatalytic process as a whole [1]. The $MV^{2+}$ has a good solubility in water, stability towards chemical and photochemical destruction and the pH-independent one-electron reduction potential ($E^0 = -0.44$ V vs. normal hydrogen electrode, NHE) [1]. At the same time, the cation-radical $MV^{\bullet+}$ is characterized by strong absorption bands in the UV and visible spectral range, the fact allowing to study the kinetics of the photocatalytic process using the optical spectroscopic techniques.

The photocatalytic reduction of $MV^{2+}$ was probably one of the first photoprocesses studied for nanometer semiconductor crystals [2]. This reaction was used to evaluate the photocatalytic properties of colloidal CdS [3–10], $In_2S_3$ [9], and Se NCs [11] stabilized in polymer solutions, CdS NCs incorporated in the lipid vesicles [7], as well as PbS NCs stabilized with aminothiophenol [12]. The photocatalytic properties in $MV^{2+}$ reduction were found for colloidal titanium dioxide NCs [1,13–16] and nanocrystalline $TiO_2$ powders [17,18].

An increase of the quantum efficiency of $MV^{2+}$ reduction with the decrease of CdS NCs size [3] is one of the first examples of the quantum size phenomena in the semiconductor photocatalysis. The relationship between the conduction band potential $E_{CB}$ of CdS NCs and the rate of $MV^{2+}$ photoreduction obtained showed the applicability of the model of energetic (thermodynamic) "design" of the semiconductor-based photocatalytic systems [1,19] not only for bulk materials but also for nanocrystalline semiconductors with size effects. In this model, an effective photocatalytic action can be achieved only when the $E_{CB}$ of a photocatalyst is more negative than the redox-potential of an acceptor A, $E_{CB} < E(A/A^{\bullet-})$, while the valence band edge potential is more positive than the redox-potential of a donor $D$, $E_{VB} > E(D/D^{\bullet+})$. The rate of interfacial electron transfer of the conduction band electrons ($e^-_{CB}$) to the acceptor and the valence band holes ($h^+_{VB}$) to the donor is determined by the respective overpotentials $\Delta E_e = E(A/A^{\bullet-}) - E_{CB}$ and $\Delta E_h = E_{VB} - E(D/D^{\bullet+})$. For the semiconductor NCs with the quan-

* Corresponding author. Tel.: +380 44 525 0270; fax: +380 44 525 0270.
*E-mail addresses:* stroyuk@inphyschem-nas.kiev.ua, alstroyuk@ukr.net (O.L. Stroyuk).

1010-6030/$ – see front matter © 2010 Published by Elsevier B.V.
doi:10.1016/j.jphotochem.2009.11.019

tum size effects this conception can be applied taking into account that $E_{CB}$ and $E_{VB}$ increase with the reduction of NC size $d$.

The results reported in the present paper show that the relationship between the quantum efficiency of the photocatalytic $MV^{2+}$ reduction and the energy of the conduction band electrons of semiconductor NCs has a general character and is valid not only at a variation of the size of semiconductor NCs in the regime of spatial exciton confinement at the constant composition of the system, but also for a much wider range of photocatalytic systems differing by the composition of colloidal semiconductor (ZnO, ZnS, $Cd_xZn_{1-x}S$, CdS, CdSe, CdTe), the NC size, as well as the type of stabilizer and electron donor.

A special attention is paid to the photocatalytic reduction of $MV^{2+}$ with the participation of CdSe NCs. The kinetic parameters of this reaction differ substantially from those of the methylviologen reduction in the presence of CdS NCs reported in [3–10], as well as ZnO and $Cd_xZn_{1-x}S$ NCs reported here. An interpretation of the differences is proposed taking into account specifics of the structure of colloidal semiconductor NCs, in particular, the nature and depth (energy) of the surface electron traps.

## 2. Experimental

Colloidal ZnO solutions in dry 2-propanol were prepared from zinc acetate and sodium hydroxide at 0 °C and aged at 55–60 °C for 2 h [20]. According to optical spectroscopy and XRD, colloidal zinc oxide solutions with $[ZnO] = 2 \times 10^{-3}$ M contain hexagonal 4.8–5.0 nm ZnO NCs [20]. The colloids were stabilized by an excess of $Zn(CH_3COO)_2$.

Colloidal $Cd_xZn_{1-x}S$ solutions ($x = 0.1$) in water were prepared from cadmium and zinc chlorides and sodium sulfide in the presence of sodium polyphosphate (SPP) as described in [21,22]. The composition of $Cd_xZn_{1-x}S$ NCs was defined by ratio $x = [CdCl_2]/([CdCl_2] + [ZnCl_2])$. According to XRD results, at $[Cd_xZn_{1-x}S] = 5 \times 10^{-3}$ M the average size NCs is 6.0–6.5 nm regardless of their composition [22]. At higher precursor concentrations larger $Cd_xZn_{1-x}S$ NCs, with $d = 10$–11 nm, can be produced.

Colloidal solutions of CdSe were prepared from $CdCl_2$ and $Na_2SeSO_3$ at $(3–5) \times 10^{-3}$ M of each reactant in aqueous gelatin solutions. Details of the synthesis can be found in [23,24].

The absorption and photoluminescence (PL) spectra were registered using the Specord 210 spectrophotometer and the Perkin-Elmer LS55 luminescence spectrometer. The illumination was performed with a mercury high-pressure 1000 W lamp equipped with an optical filter transmitting at $\lambda = 310$–370 nm (the light intensity $I = 1.0 \times 10^{15}$–$1.7 \times 10^{17}$ quanta per s) or a mercury low-pressure lamp with $\lambda = 253.7$ nm ($I = 1.0 \times 10^{15}$ quanta per s). The light intensities were measured by the ferrioxalate actinometry and varied using the calibrated wire meshes. The photochemical experiments were carried out in glass 10.0 mm optical cuvettes bubbled with argon prior to illumination. The initial quantum yield of methylviologen cation-radical formation was calculated for the initial 60-s span of illumination as $\Phi(MV^{\bullet+}) = ([MV^{\bullet+}]N_aV_{cuv}) \times (1000It)$, where $[MV^{\bullet+}]$ is the molar concentration of cation-radical, $N_a$ is the Avogardo number, $V_{cuv}$ is the cuvette volume (in mL), $t$ is the illumination time (in s). The composition of solutions exposed to illumination is given in the figure captions.

## 3. Results and discussion

Illumination of deaerated aqueous solutions containing methylviologen chloride, 2-propanol and ZnO NCs results in the formation of $MV^{\bullet+}$ cation-radical with the characteristic absorption bands at 350–400 and 550–650 nm (Fig. 1a) [1–3]. No $MV^{\bullet+}$ was detected in the dark, while the rate of photoproduct formation without ZnO NCs is smaller by an order of magnitude. The facts indicate that ZnO NCs act as a photocatalyst of the methylviologen reduction by 2-propanol. The quantum efficiency of the photocatalytic reaction is $(5–6) \times 10^{-4}$ (Fig. 1b), the rate of $MV^{\bullet+}$ formation increasing proportionally to the light intensity (inset in Fig. 1b).

The photocatalytic formation of $MV^{\bullet+}$ is also observed in colloidal $Cd_xZn_{1-x}S$ solutions ($x = 0..1$) in the presence of $Na_2SO_3$ as a sacrificial electron donor (Fig. 2a). The initial quantum efficiency of the photoprocess increases from $6 \times 10^{-4}$ for CdS NCs to $(4–5) \times 10^{-3}$ for ZnS NCs. In contrast to the ZnO NCs-based systems, $MV^{\bullet+}$ formation in the presence of $Cd_xZn_{1-x}S$ NCs becomes slower as the exposure increases. The fact can be accounted for either by blocking of the NC surface by the photoproduct or by the involvement of $MV^{\bullet+}$ in a parallel photoinduced reaction.

The initial quantum efficiency of the photocatalytic $MV^{2+}$ reduction by sodium sulfite in the presence of gelatin-stabilized colloidal CdSe NCs (Fig. 2b, curve 1) and mercaptoacetic acid-stabilized CdTe NCs [25] was found to be $2.5 \times 10^{-3}$ and $3.0 \times 10^{-3}$, respectively.

The presented experimental results allow to trace a relationship between the thermodynamic parameters of semiconductor nanophotocatalysts studied, specifically, $E_{CB}$, and the quantum efficiency of $MV^{2+}$ photoreduction. The conduction band potentials of ZnO, $Cd_xZn_{1-x}S$, and CdSe NCs depend on the NC size $d$ because of the quantum size effects and in case of $Cd_xZn_{1-x}S$ NCs also change with the composition $x$. The values of $E_{CB}(d)$ can be calculated using the electrophysical constants of corresponding bulk materials in terms of the effective masses approximation [19,26] as

$$E_{CB}(d) = E_{CB}^{bulk} - m_h^*(m_e^* + m_h^*)^{-1}\Delta E_g(d),$$

$$E_{VB}(d) = E_{VB}^{bulk} + m_e^*(m_e^* + m_h^*)^{-1}\Delta E_g(d),$$

where $\Delta E_g$ is a size-dependent increment of the band gap of nanocrystalline semiconductor ($E_g$) over the corresponding bulk value ($E_g^{bulk}$), which can be assessed from the optical spectra, $m_e^*$ and $m_h^*$ are the effective masses of electron and hole, respectively.

Taking into account that for the bulk cadmium and zinc sulfides a mismatch between the respective $E_{VB}$ potentials is small (0.2 eV) comparatively to a difference in $E_{CB}$ potentials (1.0 eV), the relationship between the $E_{VB}^{bulk}$ and composition $x$ for the bulk $Cd_xZn_{1-x}S$ crystals may be approximated by a linear combination

$$E_{VB}^{bulk}(x) = xE_{VB}^{bulk}(CdS) + (1-x)E_{VB}^{bulk}(ZnS),$$

where $E_{VB}^{bulk}(CdS) = 1.60$ V vs. NHE [19], $E_{VB}^{bulk}(ZnS) = 1.80$ V [1]. The potentials $E_{CB}^{bulk}$ can therefore be calculated as $E_{CB}^{bulk}(x) = E_{VB}^{bulk}(x) - E_g^{bulk}(x)$. The band gap $E_g^{bulk}(x)$ can be found using the well-known empirical expression $E_g^{bulk} = 3.6 - 1.78x + 0.61x^2$ [27,28]. The effective electron and hole masses for $Cd_xZn_{1-x}S$ NCs of an arbitrary composition can also be presented as linear combinations [27] $m_e^*(x) = xm_e^*(CdS) + (1-x)m_e^*(ZnS)$, $m_h^*(x) = xm_h^*(CdS) + (1-x)m_h^*(ZnS)$, where $m_e^*(CdS) = 0.20m_0$, $m_e^*(ZnS) = 0.27m_0$, $m_h^*(CdS) = 0.70m_0$, $m_h^*(ZnS) = 0.58m_0$ [29] ($m_0$ is the electron rest mass).

For zinc oxide NCs the reported values $E_{CB}^{bulk} = -0.4$ V vs. NHE at pH 7, $m_e^* = 0.26m_0$, and $m_h^* = 0.59m_0$ were used [30,31]; for CdSe NCs – $E_{CB}^{bulk} = -1.1$ V, $m_e^* = 0.13m_0$, and $m_h^* = 0.45m_0$ [29,32]. For CdTe NCs the value $E_{CB} = -1.6$ V, derived in [33] from direct electrochemical measurement in a colloidal solution of mercaptoacetic acid-stabilized CdTe NCs, was adopted.

An analysis of the data presented showed that a linear relationship exists between the initial quantum efficiency of methylviologen reduction $\Phi(MV^{\bullet+})$ and the conduction band potential of the semiconductor nanophotocatalysts (Fig. 3).

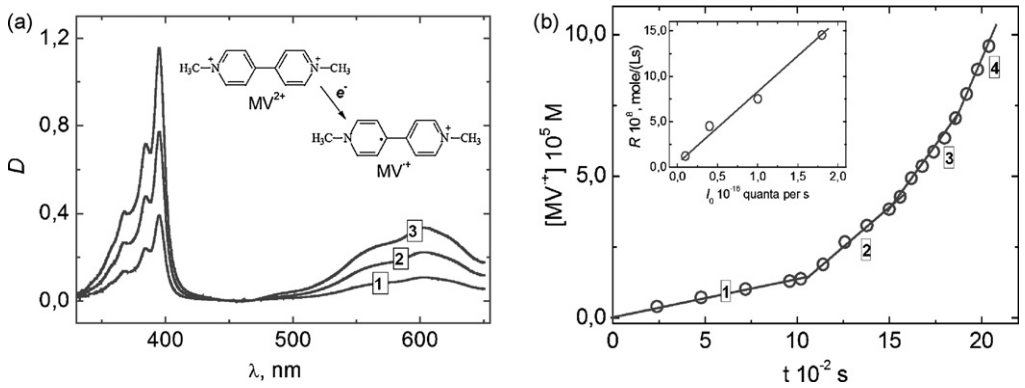


**Fig. 1.** (a) Absorption spectrum of the methylviologen cation-radical, photocatalytically produced in the presence of ZnO NCs in water/2-propanol mixture (1:1, v/v) at 1 min (curve 1), 2 min (2), and 3 min exposure (3). Inset: the structure of bication and cation-radical of methylviologen. (b) Kinetic curves of the photocatalytic formation of $MV^{\bullet+}$ in water/2-propanol mixtures in the presence of ZnO NCs. The light intensity $I = 1.0 \times 10^{15}$ quanta per s (Section 1), $4.0 \times 10^{15}$ quanta per s (2), $1.0 \times 10^{16}$ quanta per s (3), and $1.8 \times 10^{16}$ quanta per s (4). [ZnO] = $1.5 \times 10^{-3}$ M, [$MV^{2+}$] = $5 \times 10^{-4}$ M.

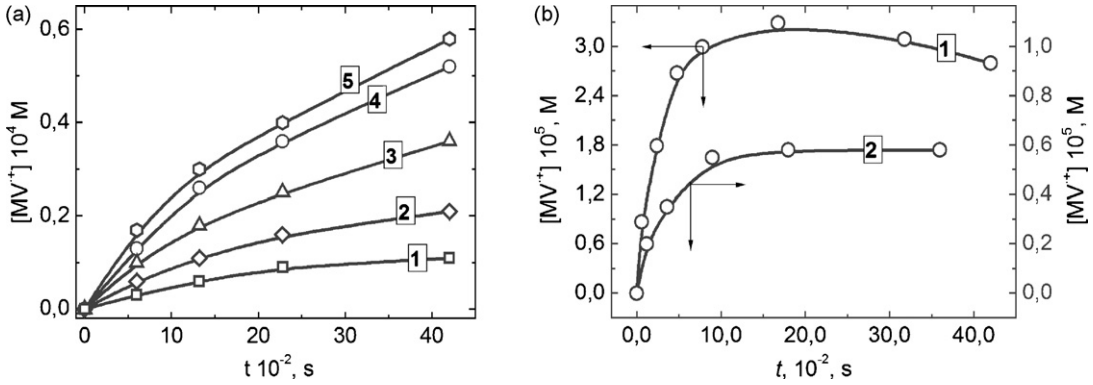


**Fig. 2.** (a) Kinetic curves of the photocatalytic formation of $MV^{\bullet+}$ in aqueous solutions in the presence of CdS NCs (curve 1), ZnS NCs (5) and $Cd_xZn_{1-x}S$ NCs with $x = 0.75$ (2), 0.5 (3), and 0.25 (4). [$Cd_xZn_{1-x}S$] = [$MV^{2+}$] = $1.0 \times 10^{-3}$ M, [$Na_2SO_3$] = $1.00 \times 10^{-2}$ M, $I = 1.0 \times 10^{15}$ quanta per s, $\lambda = 254$ nm. (b) Kinetic curves of the photocatalytic formation of $MV^{2+}$ in the presence of CdSe NCs (curve 1) and without photocatalysts (2). [CdSe] = $1.5 \times 10^{-4}$ M, [$MV^{2+}$] = $1.0 \times 10^{-3}$ M, [$Na_2SO_3$] = $1.00 \times 10^{-2}$ M, $\lambda = 310$–$370$ nm, $I = 1.7 \times 10^{17}$ quanta per s.

This relationship unites the semiconductor NCs of different compositions—zinc oxide and zinc sulfide, cadmium and cadmium-zinc sulfides, cadmium selenide and telluride. It is valid for the same semiconductor with different NC sizes (points No. 7 and 9), for different stabilizers (gelatin for No. 3 and 7, SPP for No. 1, 4-6, 8 and 9, mercaptoacetic acid in No. 2, and zinc acetate in case No. 10), as well as for the systems differing by electron donor (2-propanol in case of ZnO NCs and sodium sulfite in other cases).

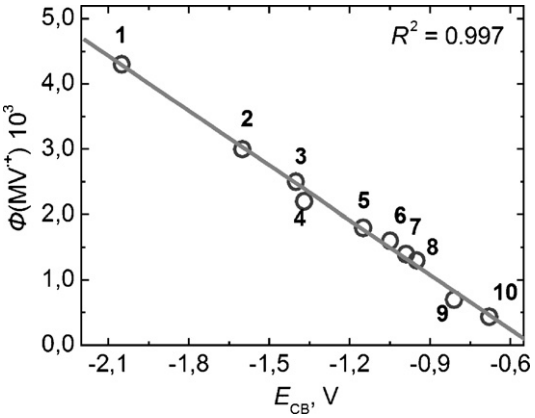


**Fig. 3.** A relationship between the initial quantum efficiency of the photocatalytic methylviologen reduction $\Phi(MV^{\bullet+})$ and the conduction band potential $E_{CB}$ of 5.0 nm ZnS NCs (point No. 1), 3.0 nm CdTe NCs (2), 5.5–5.6 nm CdSe NCs (3), $Cd_{0.25}Zn_{0.75}S$ NCs (4), $Cd_{0.50}Zn_{0.50}S$ NCs (5), $Cd_{0.63}Zn_{0.33}S$ NCs (6), and CdS NCs with the size $d = 6.5$–$6.6$ nm (7), $Cd_{0.75}Zn_{0.25}S$ (8) and CdS NCs with $d = 10$–$11$ nm (9), and 4.8 nm ZnO NCs (10). Solid line represents a linear fit of the presented data.

The linear dependence presented reflects a relationship between the rate of photoinduced interfacial electron transfer from the semiconductor NCs to $MV^{2+}$ and the overpotential of this process, $E_{CB} - E(MV^{2+}/MV^{\bullet+})$, which does not change with a variation of components of the photocatalytic system and their properties. This relationship is an example showing that the model of the design of semiconductor-based photocatalytic systems in terms of the energy parameters of the reaction participants [19] may be applied to nanocrystalline semiconductors with size effects.

A comparison of Fig. 2a and b shows the dynamics of methylviologen photoreduction in the presence of $Cd_xZn_{1-x}S$ and CdSe NCs being quite different. In particular, the rate of $MV^{\bullet+}$ formation with the participation of CdSe NCs, which is higher than in case of CdS NCs on the initial stage, gradually falls. The photoproduct concentration achieves a certain limiting value and then even falls indicating an additional reaction with the participation of $MV^{\bullet+}$ taking place in the system.

As the $MV^{\bullet+}$ concentration does not change in the dark, this parallel process is also of photochemical nature. At the same time, a difference in the shape of kinetic curves presented in Fig. 2a and b indicates that the extinction of $MV^{\bullet+}$ cation-radical does not originate exclusively from its spontaneous photochemical transformations—it requires the presence of CdSe NCs. So, this reaction, like the photoreduction of $MV^{2+}$, proceeds in the photocatalytic regime.

The conversion of $MV^{2+}$ in CdSe NCs-based systems does not exceed 10% in all cases. After adding to the solution, where the

photoreaction has stopped, a new portion of $MV^{2+}$ or CdSe NCs the concentration of $MV^{\bullet+}$ increases and achieves a new saturation limit. So, the slowdown of the photoreaction is not apparently associated with deterioration of the photocatalytic properties of CdSe NCs or with the complete consumption of $MV^{2+}$.

Oxidation of the methylviologen cation-radical by $h^+_{VB}$ also cannot be regarded as a primary reaction responsible for the extinction of $MV^{\bullet+}$ as assumed, for example, in [5,10]. Considering that the concentration of $MV^{\bullet+}$ is lower by two orders of magnitude than the concentration of $MV^{2+}$, the rates of formation and consumption of the methylviologen cation-radical can become comparable only if the rate constant of the first process ($k_1$) is smaller at least by an order of magnitude than the rate constant of the second process ($k_2$). Oxidation of $MV^{\bullet+}$ by the photogenerated holes can be regarded as one of the routes of the electron–hole recombination and, if active, at $k_1 \ll k_2$ it should efficiently suppress the photocatalytic formation of $MV^{\bullet+}$.

The colloidal selenium [24], which can appear in the system as a result of oxidative photocorrosion of CdSe NCs and capable of radical scavenging [11], was found to have no effect either on the formation rate or on the limiting concentration of $MV^{\bullet+}$.

A "plateau" on the kinetic curves of $MV^{\bullet+}$ formation is typical not only for the photocatalytic $MV^{2+}$ reduction but also to the photochemical reduction of methylviologen by sodium sulfite without additional photocatalysts (Fig. 2b, curve 2). It was shown in [10,34] to originate from the reduction of $MV^{\bullet+}$ to $MV^0$ at photoexcitation of the cation-radical dimer:

$$2MV^{\bullet+} \Leftrightarrow (MV^{\bullet+})_2 \quad (1)$$

$$(MV^{\bullet+})_2 + h\nu \rightarrow MV^{2+} + MV^0 \quad (2)$$

Transformation of $MV^{\bullet+}$ to $MV^0$ was also observed at the photocatalytic $MV^{2+}$ reduction with the participation of $Ru(bpy)_3^{3+}$ [35]. Considering these facts, the photocatalytic reduction of $MV^{\bullet+}$ to $MV^0$ in the CdSe NCs-based systems can also be assumed to be responsible for the extinction of methylviologen cation-radical.

The conduction band electrons of CdS and CdSe NCs have high enough potential to reduce $MV^{2+}$ to $MV^{\bullet+}$ (Fig. 4). At the same time, only CdSe NCs can provide a sufficient driving force for the further reduction of $MV^{\bullet+}$ to $MV^0$. The cadmium sulfide NCs with $E_{CB} = -0.95$ V vs. NHE can participate in this process only in the state of photoinduced polarization when the charging of NCs by electrons increases the $e^-_{CB}$ energy by hundreds of meV [36].

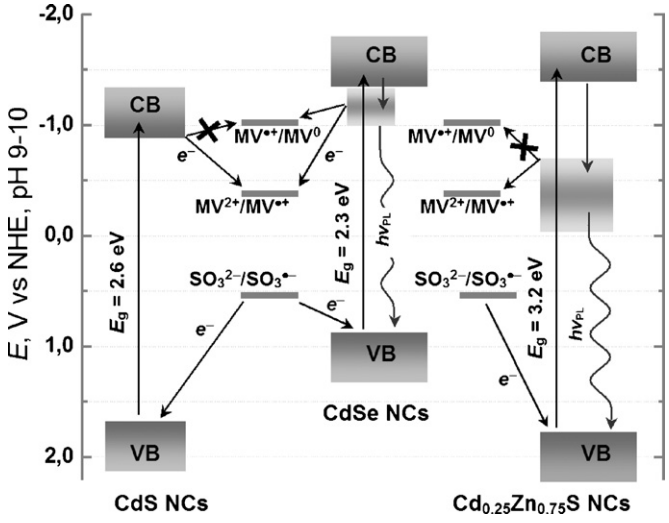


**Fig. 4.** A scheme illustrating the electron transitions in the system composed of semiconductor NCs (CdS, CdSe, $Cd_{0.25}Zn_{0.75}S$), $MV^{2+}$, $MV^{\bullet+}$ and sodium sulfite. $h\nu_{PL}$—a PL quantum.

This interpretation, however, cannot explain the differences in the kinetics of $MV^{\bullet+}$ formation for the other couple of semiconductors – CdSe and $Cd_{0.25}Zn_{0.75}S$ NCs with close $E_{CB}$ levels – −1.40 and −1.45 V for selenide and sulfide semiconductor, respectively. This seeming contradiction calls for the adaptation of the "classical" energy diagram of the photocatalytic system, where only $E_{CB}$ and $E_{VB}$ levels of the photocatalysts are taken into account, to the specifics of nanocrystalline semiconductors. In case of semiconductor NCs having a high and rich in defects specific surface area, of great importance becomes the surface trapping of the photogenerated charge carriers. The trap-mediated interfacial charge transfer can effectively compete with $MV^{\bullet+}$ for the conduction band electrons.

The depth relative to $E_{CB}$ and $E_{VB}$ levels and the energy distribution of charge traps can be evaluated from the luminescence spectra of the nanophotocatalysts. Colloidal $Cd_xZn_{1-x}S$ and CdSe NCs have broad PL bands shifted to longer wave-lengths from the respective absorption band edges (Fig. 5). A substantial Stokes shift and a large spectral width of the PL band suggest that the radiative recombination involves the surface-trapped charge carriers with a broad energy distribution. The investigation of PL properties of colloidal $Cd_xZn_{1-x}S$ [37] and CdSe NCs [23,24] showed that the luminescence originates primarily from recombination of the valence band hole with the electron in a deep trap. The localized states associated with the surface traps and lying in the band gap are depicted in Fig. 5 as the sub-bands with the center and width corresponding to the maximum and spectral width of the PL bands of CdSe and $Cd_{0.25}Zn_{0.75}S$ NCs.

The photogenerated electrons that avoided the non-radiative recombination and interfacial transfer to $MV^{2+}$ are trapped on the surface of the nanophotocatalysts and lose the energy equal to the trap depth. The average energy loss increases from 0.2 eV in case of CdSe NCs to 0.6 eV for CdS and 1.0 eV for $Cd_{0.25}Zn_{0.75}S$ (Fig. 4). The chemical potential of the trapped electron in $Cd_{0.25}Zn_{0.75}S$ NCs is apparently too low for $MV^{\bullet+}$ reduction but nevertheless sufficient for reduction of $MV^{2+}$ to the cation-radical. In case of CdSe NCs the potential of trapped electron, $e^-_{tr}$, remains high enough for reduction of both $MV^{2+}$ (3), and $MV^{\bullet+}$ (4).

$$e^-_{tr} + MV^{2+} \rightarrow MV^{\bullet+} \quad (3)$$

$$e^-_{tr} + MV^{\bullet+} \rightarrow MV^0 \quad (4)$$

The rates of reactions (3) and (4) can be expressed as

$$R_1 = k_1([MV^{2+}]_0 - [MV^{\bullet+}])I_a \quad (5)$$

$$R_2 = k_2([MV^{\bullet+}])I_a \quad (6)$$

where $[MV^{2+}]_0$ is the starting methylviologen concentration, $I_a$ is the intensity of light absorbed by the nanophotocatalyst.

In the state of quasi-equilibrium, when the rates $R_1$ and $R_2$ become equal the concentration of cation-radical $[MV^{\bullet+}]_{eq}$ can be expressed as

$$[MV^{\bullet+}]_{eq} = \frac{k_1[MV^{2+}]_0}{k_1 + k_2} \quad (7)$$

By integrating the rate Eq. (8) and combining it with (7) the expression (9) for the $MV^{\bullet+}$ concentration can be obtained.

$$\frac{d[MV^{\bullet+}]}{dt} = k_1([MV^{2+}]_0 - [MV^{\bullet+}])I_a - k_2[MV^{\bullet+}]I_a \quad (8)$$

$$[MV^{\bullet+}] = [MV^{\bullet+}]_{eq} \times (1 - e^{-I_a(k_1+k_2)t}) \quad (9)$$

A linear dependence between the $\log([MV^{\bullet+}]_{eq} - [MV^{\bullet+}])$ and the exposure time $t$ anticipated by Eq. (9) is supported by the experimental results. For example, Fig. 6a shows the kinetic curves of the photocatalytic $MV^{\bullet+}$ formation at different $[MV^{2+}]_0$. From the slope of these curves presented as $\log([MV^{\bullet+}]_{eq} - [MV^{\bullet+}])$ vs. $t$ (inset in

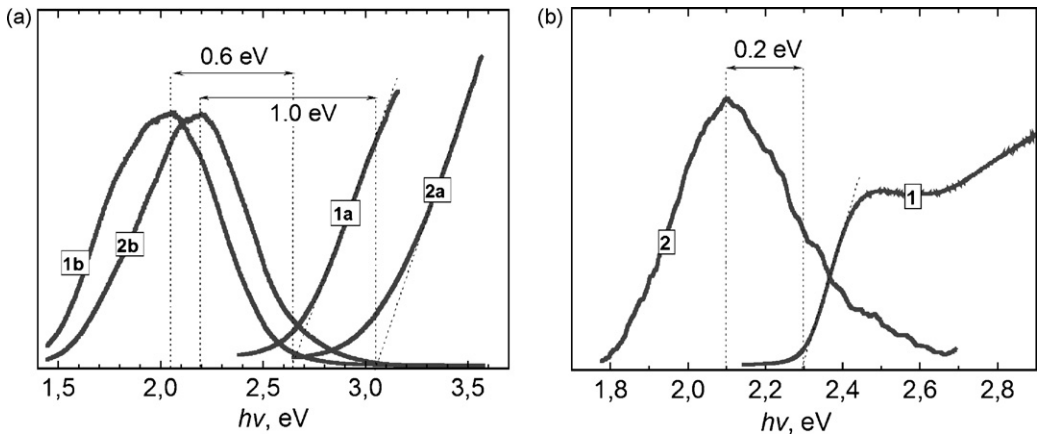


**Fig. 5.** (a) Normalized absorption (curves 1a, 2a) and PL spectra (1b, 2b) of aqueous SPP-stabilized colloidal solutions of CdS (1) and $Cd_{0.25}Zn_{0.75}S$ (2). (b) Normalized absorption (curve 1) and PL spectra (2) of gelatin-stabilized colloidal CdSe solution.

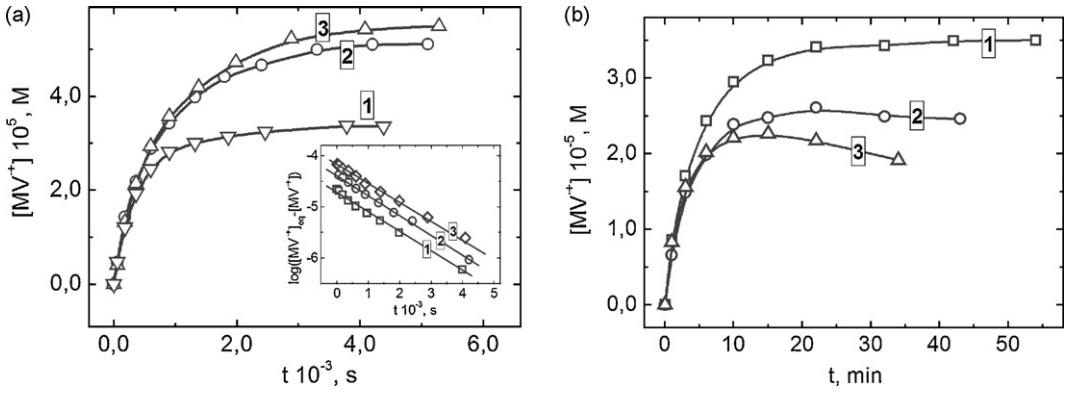


**Fig. 6.** (a) Kinetic curves of the photocatalytic reduction of $MV^{2+}$ by sodium sulfite in the presence of CdSe NCs at $[MV^{2+}]_0 = 7.5 \times 10^{-4}$ (1), $1.0 \times 10^{-3}$ (2), and $1.5 \times 10^{-3}$ M (3). Inset: the curves 1, 2, 3 presented as $\log([MV^{\bullet+}]_{eq} - [MV^{\bullet+}])$ vs. $t$. Points represent experimental data, solid lines—linear fits. (b) Kinetic curves of the photocatalytic formation of $MV^{\bullet+}$ in colloidal CdSe solutions with a different gelatin content −0.07 mass% (curve 1), 0.12 mass% (2), and 0.20 mass% (3). $[CdSe] = 1.0 \times 10^{-4}$ M, $[MV^{2+}] = 1.0 \times 10^{-3}$ M, $[Na_2SO_3] = 1.00 \times 10^{-2}$ M, $I = 1.7 \times 10^{17}$ quanta per s.

Fig. 6a) using Eq. (7) the rate constants $k_1$ and $k_2$ were found to be $k_1 = (4.2 \pm 1.2) \times 10^2$ and $k_2 = (9.0 \pm 2.0) \times 10^3$ $s^{-1}$.

This simplified kinetic scheme, though describing well the photocatalytic system at a variation of methylviologen and $Na_2SO_3$ concentration and the light intensity, has some limitations when other parameters of the system are concerned. It was found that $[MV^{\bullet+}]_{eq}$ increases from $3 \times 10^{-5}$ to $8 \times 10^{-5}$ M with an increase in CdSe concentration from $2.5 \times 10^{-5}$ to $2.0 \times 10^{-4}$ M. The fact of an equilibrium shift with the change of nanophotocatalyst concentration indicates that some process producing additional amount of $MV^{\bullet+}$ is not taken into account by the kinetic scheme. It can be, for example, oxidation of $MV^0$ by $h^+_{VB}$ (10), which gains in probability with the increase in the semiconductor concentration.

$$h^+_{VB} + MV^0 \rightarrow MV^{\bullet+} \quad (10)$$

The kinetic scheme does not take into account the viscosity of the colloidal solution. It was found that an increase in the gelatin concentration and viscosity of the solution result in a decrease of $[MV^{\bullet+}]_{eq}$ and acceleration of the process (4) (Fig. 6b). The estimations showed $k_2$ growing three times with the polymer content increased from 0.07 to 0.20 mass%. At the same time, this fact speaks in favor of the proposed kinetic scheme. The increase in viscosity of the colloidal solution should slow down both the diffusion of $MV^{2+}$ to the surface of CdSe NCs and the desorption of $MV^{\bullet+}$ from the nanophotocatalyst facilitating reaction (4).

## 4. Conclusions

A linear relationship between the conduction band potential of a number of semiconductor NCs ($Cd_xZn_{1-x}S$, CdSe, CdTe, ZnO) and the quantum efficiency of the photocatalytic methylviologen reduction was found. This relationship reflects dependence between the rate of photoinduced interfacial electron transfer from semiconductor NCs to $MV^{2+}$ and the driving force (overpotential) of this process. It has a general character and is not affected by variations in the chemical composition or size of a photocatalyst, as well as by the nature of sacrificial electron donor or the stabilizer of colloidal semiconductor.

Colloidal CdSe NCs were shown to be efficient photocatalyst of methylviologen reduction by sodium sulfite. The character of kinetics of the photoproduct ($MV^{\bullet+}$) formation is different for CdSe and $Cd_xZn_{1-x}S$ NCs. The differences are interpreted as a result of the second reaction-photocatalytic reduction of $MV^{\bullet+}$ to neutral $MV^0$ taking place with the participation of CdSe NCs.

A low efficiency of this reaction in case of $Cd_xZn_{1-x}S$ NCs can result from the fact that the photogenerated conduction band electrons are trapped on the surface of NCs before the interfacial transfer to $MV^{2+}$. The electron traps are much deeper in $Cd_xZn_{1-x}S$ NCs as compared with CdSe NCs and do not allow the trapped electron to reduce $MV^{\bullet+}$.

The presented results show that the interpretation and prediction of the photocatalytic properties of nanocrystalline semiconductors require a combined analysis of the thermodynamic

characteristics of a semiconductor, in particular, the $E_{CB}$ and $E_{VB}$ levels, together with the spectral data on the nature, concentration and energy of the surface defects, which act as the traps of the photogenerated charge carriers and contribute greatly to the specifics of the photocatalytic behavior of semiconductor NCs.

## References


[1] M. Grätzel (Ed.), Energy Resources through Photochemistry and Catalysis, Academic Press, New York, 1983.
[2] A. Henglein, J. Phys. Chem. 86 (1982) 2291–2293.
[3] H. Matsumoto, H. Uchida, T. Matsunaga, K. Tanaka, T. Sakata, H. Mori, H. Yoneyama, J. Phys. Chem. 98 (1994) 11549–11556.
[4] W.J. Albery, G.T. Brown, J.R. Darwent, E. Saeivar-Iranizad, J. Chem. Soc. Faraday Trans. 1 (81) (1985) 1999–2007.
[5] R. Rossetti, L.E. Brus, J. Phys. Chem. 90 (1986) 558–560.
[6] Y. Nosaka, M.A. Fox, J. Phys. Chem. 90 (1986) 6521–6522.
[7] H.-C. Youn, Y.-M. Tricot, J.H. Fendler, J. Phys. Chem. 91 (1987) 581–586.
[8] Y. Nosaka, H. Miyama, M. Terauchi, T. Kobayashi, J. Phys. Chem. 92 (1988) 255–256.
[9] Y. Nosaka, N. Ohta, H. Miyama, J. Phys. Chem. 94 (1990) 3752–3755.
[10] L. Meahcov, I. Sandu, J. Fluor. 14 (2004) 181–185.
[11] N.M. Dimitrijević, P.V. Kamat, Langmuir 4 (1988) 782–784.
[12] T. Torimoto, T. Sakata, H. Mori, H. Yoneyama, J. Phys. Chem. 98 (1994) 3036–3043.
[13] N. Serpone, D.K. Sharma, J. Moser, M. Grätzel, Chem. Phys. Lett. 136 (1987) 47–51.
[14] G. Grabner, R.M. Quint, Langmuir 7 (1991) 1091–1096.
[15] D. Fitzmaurice, H. Frei, J. Rabani, J. Phys. Chem. 99 (1995) 9176–9181.
[16] T. Sagawa, M. Kotani, H. Nada, X. Ji, K. Yoshinaga, K. Ohkubo, Chem. Lett. 32 (2003) 962–963.
[17] J.L. Ferry, W.H. Glaze, J. Phys. Chem. B 102 (1998) 2239–2244.
[18] H. Park, W. Choi, J. Phys. Chem. B 108 (2004) 4086–4093.
[19] A.I. Kryukov, S.Ya. Kuchmiy, V.D. Pokhodenko, Theor. Exp. Chem. 36 (2000) 69–89.
[20] A.L. Stroyuk, V.V. Shvalagin, S.Ya. Kuchmiy, J. Nanoparticle Res. 9 (2007) 427–440.
[21] A.L. Stroyuk, I.V. Sobran, A.V. Korzhak, A.E. Raevskaya, S.Ya. Kuchmiy, Colloid Polymer Sci. 286 (2008) 489–498.
[22] A.E. Raevskaya, A.L. Stroyuk, A.I. Kryukov, S.Ya. Kuchmiy, Theor. Exp. Chem. 42 (2006) 168–172.
[23] A.E. Raevskaya, A.L. Stroyuk, S.Ya. Kuchmiy, Yu.M. Azhniuk, V.M. Dzhagan, M.Ya. Valakh, Theor. Exp. Chem. 42 (2006) 150–155.
[24] A.E. Raevskaya, A.L. Stroyuk, S.Ya. Kuchmiy, Yu.M. Azhnyuk, V.M. Dzhagan, V.O. Yukhimchuk, M.Ya. Valakh, Colloids Surfaces A 290 (2006) 304–309.
[25] M.V. Kovalenko, M.I. Bodnarchuk, A.L. Stroyuk, S.Ya. Kuchmiy, Theor. Exp. Chem. 40 (2004) 215–219.
[26] L.E. Brus, J. Phys. Chem. Sol. 59 (1998) 459–465.
[27] B.A. Korgel, H.G. Monbouquette, Langmuir 16 (2000) 3588–3594.
[28] D.V. Petrov, B.S. Santos, G.A.L. Pereira, C. de Mello Donegá, J. Phys. Chem. B 106 (2002) 5325–5334.
[29] Landolt-Bornstein (Numerical data and functional relationships in science and technology) — Group III: Condensed Matter, Vol. 41. – Berlin:Springer. - 2006.
[30] D.W. Bahnemann, C. Kormann, M.R. Hoffmann, J. Phys. Chem. 91 (1987) 3789–3798.
[31] E.M. Wong, P.G. Hoertz, C.J. Liang, B.-M. Shi, G.J. Meyer, P.C. Searson, Langmuir 17 (2001) 8362–8367.
[32] W. Ho, J.C. Yu, J. Mol. Catal. A 247 (2006) 268–274.
[33] T. Nakashima, M. Sakashita, Y. Nonoguchi, T. Kawai, Macromolecules 40 (2007) 6540–6544.
[34] H. Feilchenfeld, G. Chumanov, T.M. Cotton, J. Phys. Chem. 100 (1996) 4937–4943.
[35] B. Ferrer, F.X. Llabrés i Xamena, H. García, Inorg. Chim. Acta 360 (2007) 1017–1022.
[36] A.L. Stroyuk, A.I. Kryukov, S.Ya. Kuchmiy, V.D. Pokhodenko, Theor. Exp. Chem. 41 (2005) 67–87.
[37] A.L. Stroyuk, V.M. Dzhagan, S.Ya. Kuchmiy, M.Ya. Valakh, D.R.T. Zahn, C. von Borczyskowski, Theor. Exp. Chem. 43 (2007) 275–281.